Energy 286 (2024) 129566

Contents lists available at ScienceDirect

Energy

journal homepage: www.elsevier.com/locate/energy

Forecasting electricity production from various energy sources in Türkiye: A predictive analysis of time series, deep learning, and hybrid models

Emrah Gulay *, Mustafa Sen, Omer Burak Akgun

Department of Econometrics, Dokuz Eylul University, Izmir, Turkiye

ARTICLE INFO

Keywords:
Forecasting
Time series analysis
Deep learning models
Hybrid models
Electricity production
Renewable energy sources

ABSTRACT

When it comes to energy sources used in electricity production, the future forecasting of electricity production from renewable energy sources is highly important for both the success of technological advancements in the renewable energy field and energy security. To forecast electricity production from renewable energy sources reliably, it is necessary to accurately model the components of the relevant series. The central argument of this paper is that the various components derived from electricity production data, particularly the residual component, retain valuable predictive information despite their intricate and nonlinear nature. While linear modelling may be highly accurate initially, repeating residuals within linear structures is a discrepancy in terms of data type and methodology. In this paper, different types of hybrid models that combine a decomposition method and both machine learning and statistical approaches are suggested for forecasting electricity production from different energy sources.

1. Introduction

The lack of access to energy has a direct impact on the welfare, health, and food security of both nations and individual households [1,2]. The meaning of energy poverty differs depending on a country's level of development. In less developed countries, energy poverty is described as ineffective access to renewable energy sources, whereas in more developed countries, it is defined as household energy costs that adversely impact households because of factors such as high energy prices, low household incomes, and ineffective energy usage [3]. The global emphasis is on the significance of moving towards various renewable energy sources that provide environmental benefits by reducing reliance on fossil fuels and improving social welfare. The rapid depletion of fossil fuels, an exhaustible resource that causes air pollution and serious health problems, is one of the key reasons for transitioning towards diverse renewable energy sources [4].

Türkiye, like other countries, aims to increase the variety of its energy sources by investing in renewable energy technologies such as wind, solar, biomass, and hydropower, prompted by the oil crises of the 1970s. The key objective of these endeavours is to replace fossil fuels with renewable energy alternatives and achieve energy security, environmental stability, and sustainable development goals.

The production of electricity affects not only a country's development and growth but also the environment and people's quality of life [5]. The growing demand for electricity due to the increasing population requires Türkiye to have a stable and sustainable economic structure. Additionally, due to the negative impact of non-renewable energy sources on air quality and climate, interest in different renewable energy sources is expected to increase. According to the Türkiye National Energy Plan, in 2022, the production of electricity was derived from various resources, with coal being the largest contributor at 34.6%, followed by natural gas at 22.2%, hydropower at 20.6%, wind at 10.8%, solar at 4.7%, geothermal at 3.3%, and other sources at 3.7%. Global electricity production relies heavily on fossil fuels. However, the sources of electricity production, whether fossil or renewable, are equally important as access to electricity when considering sustainable development goals. The impact of various energy sources used in electricity production on energy poverty is not only direct but also indirect, as these sources affect energy poverty through price, employment, and CO_2 emissions [6]. Accurately predicting the contributions of fossil and renewable energy sources to future electricity production is crucial in Türkiye. Studies by the Ministry of Energy and Natural Resources on energy source shares in electricity production for 2028 under the National Energy and Mining Policy suggest an increase in renewable energy source shares, mainly wind and solar energy. Accurate prediction of the shares of renewable energy sources used in electricity production can lead to reduced fossil fuel imports and contribute to the country's economy, according to reports for 2028.

This paper makes two main contributions to the existing literature. First, the aim is to determine the model with the highest forecast accuracy in modelling and forecasting electricity production from both

* Corresponding author.
E-mail addresses: emrah.gulay@deu.edu.tr (E. Gulay), mustafasen@live.nl (M. Sen), akgunburakomer@gmail.com (O.B. Akgun).

https://doi.org/10.1016/j.energy.2023.129566
Received 7 June 2023; Received in revised form 18 September 2023; Accepted 1 November 2023
Available online 4 November 2023

fossil and renewable energy sources. To attain this objective, the study employs a combination of approaches that entail the separate modelling and forecasting of the individual components of time series and the implementation of time series models and deep learning models. The study uses not only time series models and deep learning models but also hybrid approaches (see Figs. 1 and 2). Second, from an academic standpoint, selecting the most performant model developed based on energy data will enable researchers in this field to identify the best model with their data. This, in turn, is expected to enhance the number and effectiveness of studies in this area.

1.1. Dealing with limitations in forecasting models

In numerous research endeavours focusing on electricity production forecasted from diverse energy sources in Türkiye, prevailing methodologies encompass the use of artificial neural network (ANN) models alongside fundamental univariate time series models. The reliance solely on computational intelligence methods for forecasting purposes is inadequate in terms of forecast accuracy, given the dependency of electricity production data on factors such as the region, energy source type (renewable or non-renewable), and diverse local factors. Their ability to forecast can be limited because of their insufficient efficiency in identifying the characteristics of nonlinear time series, particularly since they are ineffective in grasping the dynamics of nonlinear time series.

To overcome this issue, the proposed hybrid approach uses not only univariate time series models but also deep learning models, leveraging the seasonal and trend decomposition using the Loess (STL) decomposition method that allows for extracting meaningful components from nonlinear time series. This hybrid approach involves modelling and forecasting each component individually, which enables a thorough analysis, improves the modelling process, and enhances the accuracy of forecasts. As a result, it leads to a deeper understanding of the nonlinear processes underlying the time series.

1.2. The novelty of the study

The research's contribution to the existing literature can be summarized as follows:

- Developing an approach that yields higher forecasting accuracy compared to univariate time series models, multivariate regression models with various inputs, and deep learning models by using different scenarios such as autoregressive models or models with features, which can serve as a fundamental method for forecasting electricity production data obtained from diverse energy sources.
- Unlike previous studies on electricity production forecasting in Türkiye, this research aims to provide a detailed comparison not only in terms of the types of energy sources used but also regarding the time series models employed, including deep learning models and a hybrid approach.
- Finally, errors in nonlinear time series may contain important information such as noise, irregularities, and nonlinear dynamics. Analysing these errors properly can help identify hidden patterns and structures; and therefore, a detailed analysis of errors has been carried out for each piece of electricity production data.

In forecasting studies, various explanatory variables related to the relevant time series are used as inputs to enhance forecast accuracy, especially in econometric and machine learning models. However, such forecasting processes, in addition to offering an arbitrary approach to variable selection, have some disadvantages in terms of time and computational complexity due to the increase in the number of inputs in the analyses. Therefore, the primary objectives of this paper are to shed light on the characteristics of time series components in the context of forecasting and to introduce a hybrid approach that incorporates both linear and nonlinear components, each predicted using corresponding methodologies. The central argument advanced in this paper centres on the concept that, through the decomposition of electricity production data generated from different energy sources into their components, particularly due to the significant predictive information within the residuals, the final forecasts obtained by modelling and forecasting each component are more accurate compared to the forecasts derived from either directly modelling and forecasting the electricity production data or modelling and forecasting them with the aid of explanatory variables. A comprehensive comparison has been conducted to validate the effectiveness of the proposed algorithms in forecasting electricity production data, involving not only univariate time series models and the corresponding lagged data as inputs for machine learning algorithms but also using different explanatory variables, encompassing both the autoregressive distributed lag (ARDL) model and machine learning algorithms' forecasting performance. To this end, the study uses the following algorithms. The results demonstrate that the proposed approach leads to a significant improvement in predictive accuracy when applied to out-of-sample (holdout) datasets. The use of the proposed algorithms has improved forecast accuracy, not only demonstrating lower error metrics but also providing compelling evidence that the rank-order comparisons favour their selection.

In addition to the proposal aimed at improving the accuracy of electricity production forecasting, to the best our knowledge, this study is a pioneering work in the field of forecasting electricity production in Türkiye, in terms of both the diversity and quantity of different renewable and non-renewable energy sources used.

The subsequent sections of the paper are structured as follows. Section 2 presents an overview of the literature on forecasting renewable energy. Section 3 presents details about the datasets used and the methods employed in the study. Section 4 reports the empirical findings of the study, followed by a discussion of these findings and their policy implications. Finally, in Section 5, the conclusion and insights are provided with the inclusion of future research directions.

2. Literature

Recent studies on forecasting electricity consumption have shown an increasing use of hybrid approaches combining linear time series models with machine learning algorithms [7,8] rather than relying solely on individual predictive performance of machine learning models [9]. Furthermore, interest is increasing in studies aimed at improving forecasting accuracy by combining different forecasting models based on deep learning algorithms [10]. In addition, many scholars use decomposition methods in forecasting studies based on energy-related data such as carbon prices [11], solar radiation [12], wave power [13], gasoline consumption [14], and energy prices [15], but these methods are rarely mentioned in the context of electricity production forecasting. Moreover, in studies employing dynamic forecasting models to forecast energy-related data, these data are often based on oil prices [16] and carbon emissions [17] rather than electricity production.

In Türkiye, particularly when considering the shares of energy sources in total electricity production, there is an evident shift from non-renewable to renewable energy sources in electricity production [18]. The primary reason for this shift is that renewable energy-based electricity production systems reduce carbon emissions by varying amounts for the same level of total electricity production [19]. Thus, an increasing number of researchers have shown interest in studies related to the forecasting of renewable energy. Due to this increasing interest, various models have been applied for the forecasting of renewable energy. This section particularly focuses on discussions related to forecasting various renewable energy sources used for electricity production in recent years.

Here, the forecasting studies related to energy in the literature are categorized into three groups: time series models, machine learning models, and hybrid models.

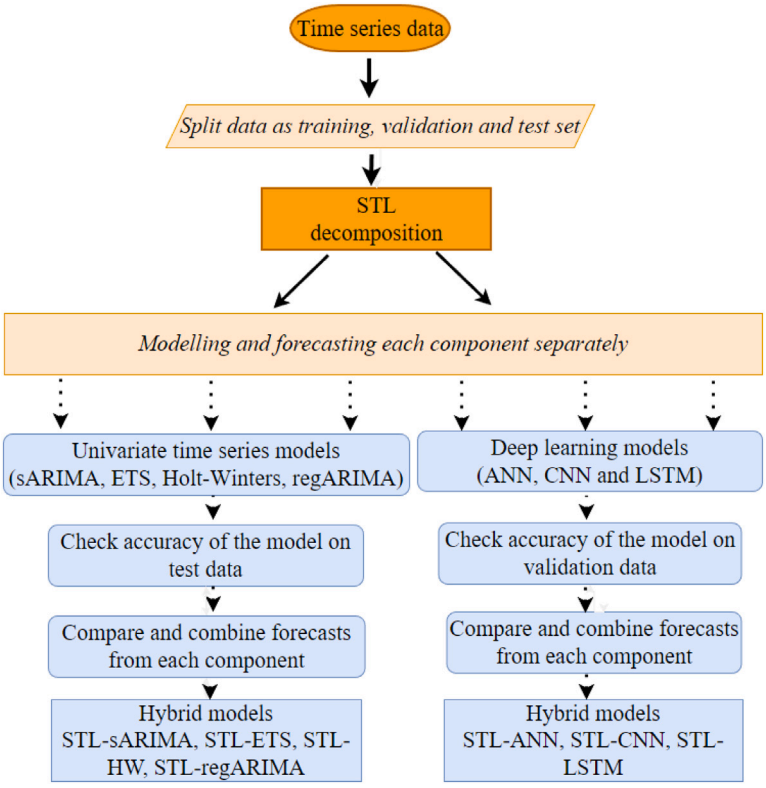

Fig. 1. The illustration of hybrid algorithm.

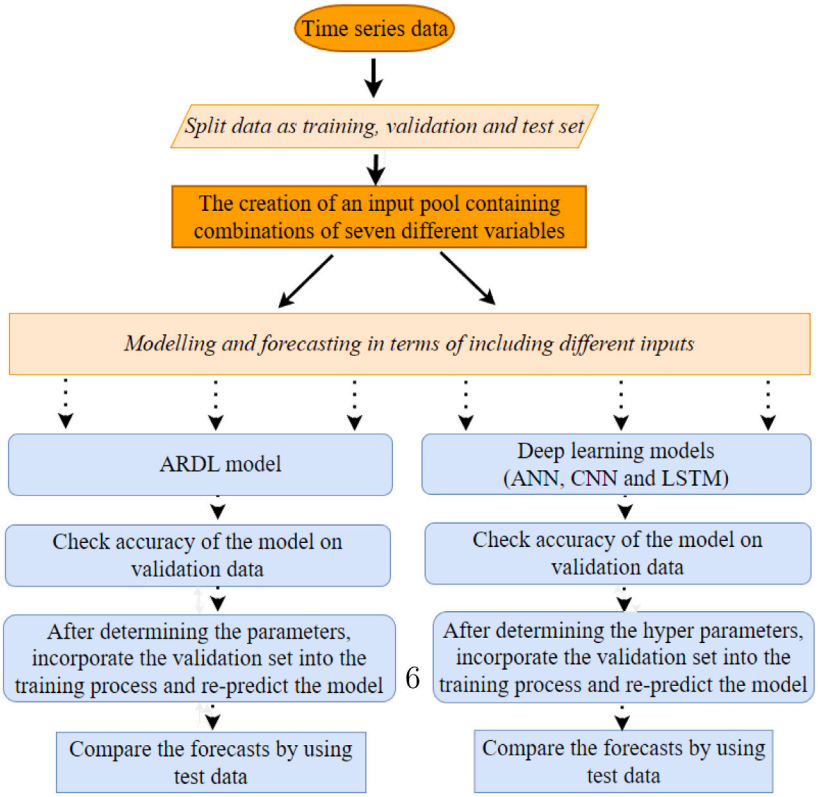

Fig. 2. The illustration of multivariate models.

2.1. Time series models

The statistical models are entirely mathematical, and their main aim is to identify relationships or patterns in the collected historical data. The study by [20] uses the autoregressive integrated moving average (ARIMA) model to model and forecast the monthly consumption of domestic electric energy in the Eastern Province of Saudi Arabia. [21] employ the ARIMA model to model and forecast future energy production and consumption in Asturias. [22] explore various univariate modelling techniques and aim to generate a one-step-ahead forecast for the monthly consumption of electric energy in Lebanon. [23] focus on different forecasting horizons to forecast wind power production by using the ARIMA model. [24] employ the ARDL model to forecast electricity consumption in Italy. [25] use the Holt–Winters (HW) exponential smoothing technique to forecast non-residential electricity consumption in Romania. They conclude that the accuracy of HW predictions is satisfactory for the time horizon evaluated in their research. [26] uses the ARDL model to forecast the electricity consumption in Cyprus up to 2030. The model employs macroeconomic variables, prices, and weather conditions as inputs to predict consumption. [27] employ the conventional ARIMA model to forecast wind power production. [28] use the ARIMA model to forecast China's primary energy consumption. [29] use the ARIMA model to forecast the daily total solar energy production from solar panels.

2.2. Machine learning models

Recent years have seen the widespread adoption of machine and deep learning models in studies related to energy forecasting. Machine learning models have gained popularity due to their ability to apply statistical accuracy and nonlinear models. [30] employ ANNs to forecast electricity spot prices. [31] put forward the use of a deep learning framework to forecast electricity demand. [7] forecast net electricity consumption using ARIMA and least-square support vector machines (LS-SVM). [32]'s study use a range of machine learning algorithms to make forecasts regarding energy demand and renewable energy production. [33] uses machine learning approaches to forecast short- and long-term electricity loads, which are of great significance in the context of energy production system planning. [34] use the long short-term memory (LSTM) model from deep learning approaches for forecasting the energy production of a solar photovoltaic plant.

2.3. Hybrid models

Recently, studies in the field of forecasting have demonstrated that the accuracy of forecasts can be enhanced by merging statistical models with both ANN models and deep learning models [35]. Considering the effectiveness in improving forecast accuracy, the hybrid approach combines the ARIMA model with methods such as Fourier transformation [36], Wavelet transformation [37,38], and support vector regression (SVR) [39]. [40] use state space models (ETS) based on the ANN model to increase forecast accuracy. [41]'s research use a hybrid approach for forecasting electric demand in the building sector. This approach combined wavelet decomposition with an SVR model. In [42], the combination of the empirical mode decomposition (EMD) and the evolutionary LS-SVM method is used to forecast carbon prices. The study's findings suggest that the integration of EMD and evolutionary LS-SVM models yields more reliable forecasts compared to traditional forecasting techniques. [43] show that the combination of LSTM and convolution neural network (CNN) models has better out-of-sample forecasting performances than individual models. [44] employ a hybrid approach by combining the ANN and SVR models to forecast renewable energy production. [45] improve the forecast accuracy by combining the ARDL, EMD and ANN models.

3. Data and methods

3.1. Data

This study aims to perform time series forecasting of Türkiye's electricity production using univariate, multivariate and hybrid models. The dataset consists of two main groups: electricity production via different sources defined as dependent variables and the factors that affect electricity production defined as independent variables (see Tables 1 and 2). Datasets were arranged in monthly periods, containing 125 observations from January 2012 to May 2022. Dependent variables contain eight different time series about electricity production. The total production (TP) series demonstrates the total electricity production. The rest of the dependent variables used in the study show how much electricity is produced from natural gas (NG), hydro (HYD), coal (COAL), wind (WIND), fuel oil (FO), bioenergy (BIO) and geothermal power (GEO).

The electricity production series is sourced from Energy Exchange Istanbul (EXIST). EXIST provides production data through two distinct methods: real-time production and injection quantity. Real-time production data are subject to potential changes as the settlement process remains incomplete. Hence, the study uses injection quantity data, which have undergone the settlement process and represent fixed values. The production data are measured in megawatt-hours (MWh) and are considered raw observations.

As previously mentioned, the electricity production data comprise the TP and the resources used for electricity production. Fig. 3 illustrates that the TP exhibits an upward trend and seasonal patterns, while the production resources display variations in terms of trend and seasonality based on their specific characteristics. The HYD variable is influenced by seasonal variations linked to water flow instability. Furthermore, fuel oil usage remains at relatively low levels, and coal has experienced a declining trend. On the other hand, the proportion of electricity production from renewable energy sources such as wind, geothermal, and biomass in the overall electricity production is growing. Fig. 3 also indicates the impact of the pandemic on electricity production. The interruption of the upward trend in TP is evident in March 2020. NG usage experienced a similar interruption despite not having an upward trend. Although the upward trend of coal had weakened before March 2020, it sharply declined in conjunction with the pandemic. Notably, renewable energy sources did not exhibit a downward trend. This finding can be explained by the relatively low proportion of renewable energy sources in the overall electricity production.

The independent variables represent the inputs used in the multivariate analyses. Based on a thorough review of the literature, several variables were identified as influential factors in electricity production and included in the analysis. These variables include the industrial production index (IPI), the real effective exchange rate (REER), the consumer production index (CPI), oil price (OP) (Brent/USD), oil import (OI) (measured in tonnes), CO_2 emissions (measured in micrograms (μg)/m3), and coal price (measured in kg/USD). Data for the independent variables were collected from various sources. The IPI and OI data were obtained from TURKSTAT, while REER, CPI, and OP data were sourced from the Central Bank of the Republic of Türkiye (CBRT). The coal price data were acquired from http://comtradeplus.un.org, and the CO_2 data were obtained from the Republic of Türkiye Ministry of Environment, Urbanisation, and Climate Change.

Fig. 4 illustrates the trends observed in various variables. The IPI exhibited an upward trend from 2012 to 2022 that was significantly disrupted by the effects of the pandemic in March 2020. However, the IPI quickly recovered and resumed its upward trend. On the other hand, the REER displayed a downtrend, while the CPI showed an upward trend. Both variables exhibited no clear seasonal patterns. The OP and CP variables displayed no specific trends or seasonal patterns. In contrast, CO_2 emissions showed an overall upward trend throughout the entire period, with the emergence of a seasonal pattern in the second half of 2019. Lastly, the OI variable demonstrated an upward trend with irregular fluctuations.

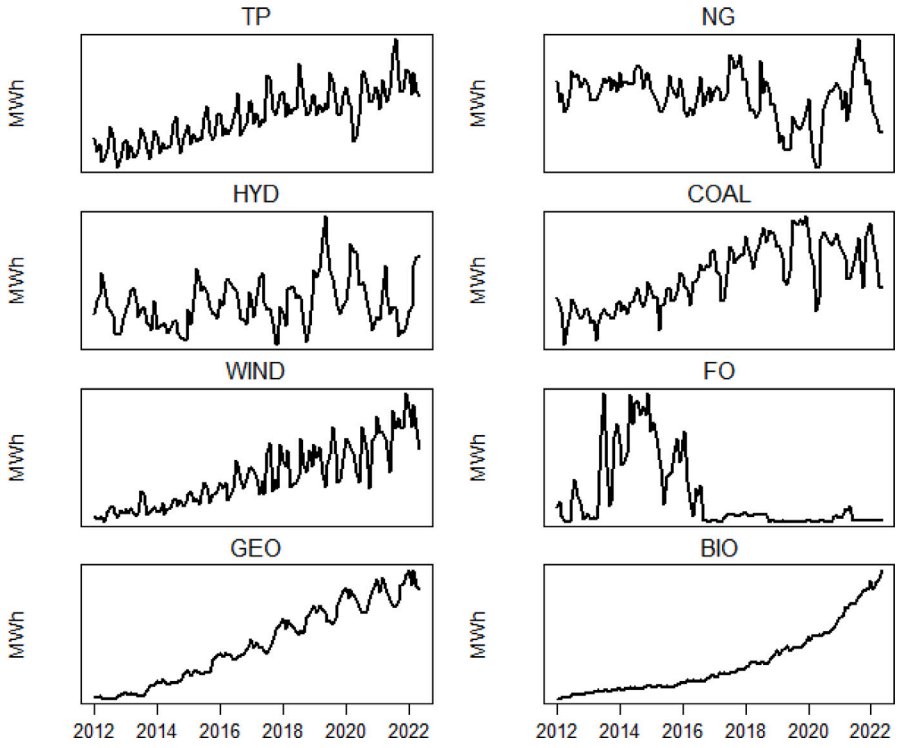

Fig. 3. Sample datasets used in the study in a monthly basis.

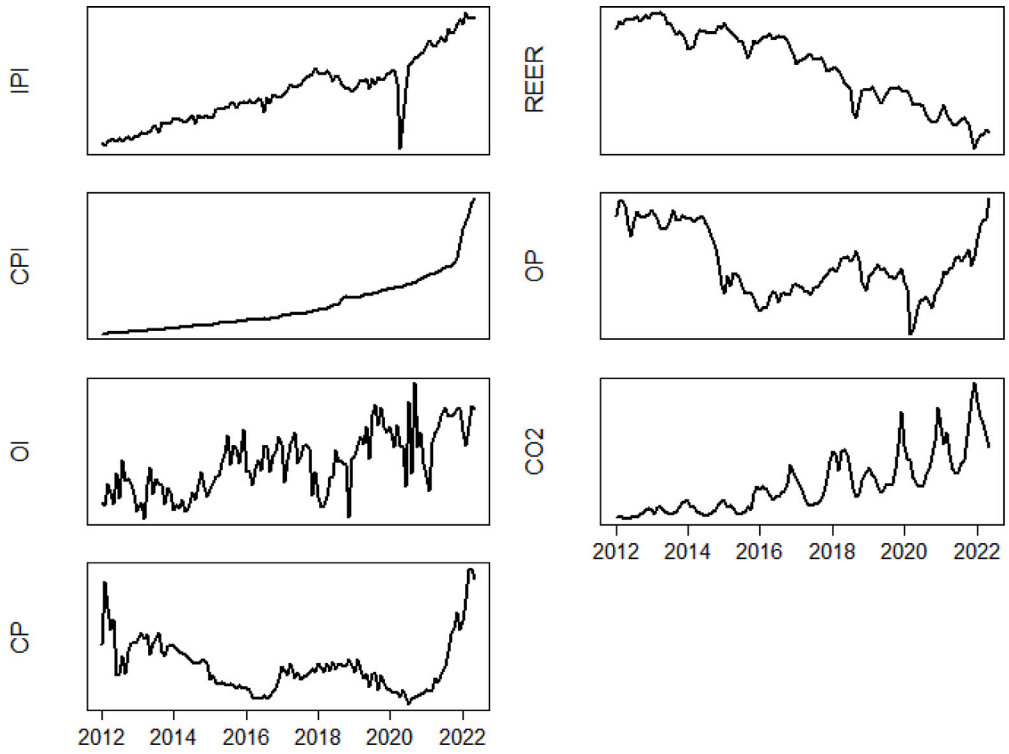

Fig. 4. Sample input variables used in the study in a monthly basis.

Table 1
Descriptive statistics for target variables.

D.S/D.V	TP	NG	HYD	COAL	WIND	FO	BIO	GEO
Mean	21 716 270	6 883 001	5265 425	6 580 417	1 409 688	122 678.3	200 471.3	403 307.9
Median	21 844 576	7 155 592	5 011 440	6 446 337	1 250 046	31 486.09	146 393	370 899.7
Maximum	30 527 152	1 162 1895	11 515 065	9 867 280	3 465 778	621 287.7	638 103.7	864 289.1
Minimum	15 961 733	1 072 281	2 237 801	2 829 847	288 446.6	299.27	28 730.31	52 292.54
Std. Dev.	3 016 242	1 947 752	1 769 645	1 734 287	770 258.4	178 556.7	156 966.8	247 488.5
Skewness	0.303356	−0.634496	0.758449	0.062323	0.549795	1.459374	1.098669	0.130195
Kurtosis	2.496615	3.637738	3.59426	1.884657	2.317255	3.801891	3.179246	1.692985
J.B Test	3.236962	10.50548	13.82358	6.560032	8.72519	47.71936	25.31471	9.250472
(Prob.)	(0.198)	(0.005)*	(0.000)*	(0.037)**	(0.012)*	(0.000)*	(0.000)*	(0.009)*
LB~Q Test	609,93	223.98	202.16	693.54	729.8	676.49	1000.2	1133.1
(Prob.)	(0.000)*	(0.000)*	(0.000)*	(0.000)*	(0.000)*	(0.000)*	(0.000)*	(0.000)*
ARCH(12)	10.132	11.88	4.91	19.6	14.87	12.128	5.297	3.2811
(Prob.)	(0.519)	(0.372)	(0.936)	(0.051)***	(0.189)	(0.354)	(0.916)	(0.986)

Note: The J-B is Jarque–Bera test for normality, LB-Q test is Ljung–Box test for 12-order autocorrelation. The ARCH (12) is Engle's test for ARCH effect. Integration shows difference level for stationary that obtained as a result of ADF (Augmented Dickey Fuller) unit root test.

* 0.01 significance level.

** 0.05 significance level.

*** 0.10 significance level.

Table 2
Descriptive statistics for input variables.

D.S/D.V	IPI	REER	CPI	OILPRC	OILIMP	CO_2	COALPRC
Mean	107.860	87.744	354.330	73.024	2 061 821.000	1 389 026.000	0.115
Median	106.460	91.600	305.240	66.780	2 049 886.000	1 139 872.000	0.105
Maximum	148.282	113.630	931.760	125.530	3 411 533.000	4 924 658.000	0.265
Minimum	79.342	47.700	201.980	14.850	1 091 171.000	154 402.600	0.054
Std. Dev.	17.060	18.483	150.846	26.683	529 252.900	1 059 048.000	0.043
Skewness	0.468	−0.378	1.610	0.292	0.248	1.115	1.379
Kurtosis	2.554	1.811	5.865	1.962	2.202	3.746	5.225
J-B Test	5.607	10.333	96.738	7.390	4.596	28.780	65.409
(Prob)	(0.060)***	(0.005)*	(0.000)*	(0.024)**	(0.100)	(0.000)*	(0.000)*
LB-Q	824.02	1072	759.59	750.4	388.18	561.17	355.17
(Prob.)	(0.000)*	(0.000)*	(0.000)*	(0.000)*	(0.000)*	(0.000)*	(0.000)*
ARCH (12)	62.2	14.84	4.95	40.1	7.85	4.11	6.98
(Prob.)	(0.000)*	(0.190)	(0.934)	(0.000)*	(0.730)	(0.967)	(0.801)

Note: The J-B is Jarque–Bera test for normality, LB-Q test is Ljung–Box test for 12-order autocorrelation. The ARCH (12) is Engle's test for ARCH effect. Integration shows difference level for stationary that obtained as a result of ADF (Augmented Dickey Fuller) unit root test.

* 0.01 significance level.

** 0.05 significance level.

*** 0.10 significance level.

3.2. Time series models

3.2.1. sARIMA model

ARIMA models are defined as integrated autoregressive-moving-average (ARMA) processes, which means they are models that handle non-stationary data.

$$\phi(B)Y_t = \phi(B)\Delta^d Y_t = \theta_0 + \theta(B)X_t \tag{1}$$

$$\phi(B) = 1 - \phi_1 B - \phi_2 B^2 - \cdots - \phi_p B^p$$

$$\theta(B) = 1 - \theta_1 B - \theta_2 B^2 - \cdots - \theta_q B^q$$

Eq. (1) shows the general form of the ARIMA (p, d, q) model. $\varphi(B)Y_t$ denotes the stationary autoregressive process and $\phi(B)\Delta^d Y_t$ denotes the nonstationary autoregressive process when the unit root operator (d) is different from zero. And $\theta(B)$ denotes the invertible moving average operator [46]. Unlike the theory series contain seasonal components in practice.

$$\phi_p(B)\Phi_p(B^s)\Delta^d\Delta_s^D Y_t = \theta_0(B)\Theta(B^S)X_t \tag{2}$$

Eq. (2) is the general multiplicative seasonal ARIMA (p, d, q)(P, D, Q)$_m$ model. The p, d, q indices are the nonseasonal orders while P, D, Q are seasonal orders [47]. In Eq. (2), Y_t is the electricity production data and X_t represents the explanatory variables which are the lagged values of Y_t. The Akaike information criterion (AIC) was used as a model selection criterion. Table 3 shows the target variables' sARIMA orders.

Table 3
The sARIMA (p, d, q)(P, D, Q)$_m$ orders.

Variables	sARIMA models
TP	$(1, 0, 0)(2, 1, 0)_{12}$
NG	$(2, 0, 0)(2, 1, 0)_{12}$
HYD	$(2, 0, 2)(1, 1, 1)_{12}$
COAL	$(2, 0, 2)(1, 1, 1)_{12}$
WIND	$(0, 0, 0)(0, 1, 1)_{12}$
GEO	$(1, 1, 0)(1, 1, 0)_{12}$
BIO	$(1, 2, 1)(1, 1, 2)_{12}$
FO	$(0, 1, 0)$

3.2.2. Holt-Winters models

Simple exponential smoothing (SES) is quite useful when datasets do not exhibit trends or seasonal patterns. If a series exhibits trend, seasonality or both, the SES method may not be able to provide accurate results. The HW method overcomes this problem by using three smoothing equation: Level (L_t), Trend (B_t) and Seasonality (S_t). The HW method can be expressed in two different forms, either additive or multiplicative, depending on how seasonality is incorporated into the model [48].

Table 4
The framework terminology of ETS models.

ETS (M, M, N)	ETS (A, M, A)	ETS (M, N, M)
ETS (M, A, N)	ETS (A, Md, N)	ETS (M, N, A)
ETS (M, A, M)	ETS (A, Md, M)	ETS (M, N, N)
ETS (A, M, N)	ETS (A, N, A)	ETS (M, A, A)
ETS (A, N, N)	ETS (M, Ad, M)	ETS (A, Ad, M)
ETS (A, A, M)	ETS (M, Ad, N)	ETS (M, M, A)
ETS (M, M, M)	ETS (M, Md, M)	ETS (A, A, A)
ETS (A, N, M)	ETS (A, Ad, N)	ETS (A, Ad, A)
ETS (A, A, N)	ETS (M, Md, A)	ETS (M, Ad, A)
ETS (A, M, M)	ETS (M, Md, N)	ETS (A, Md, A)

Multiplicative Form

$$L_t = \alpha(Y_t/S_{t-M}) + (1-\alpha)(L_{t-1} + B_{t-1}) \tag{3}$$

$$B_t = \beta(L_t - L_{t-1}) + (1-\beta)B_{t-1} \tag{4}$$

$$S_t = \gamma(Y_t/L_t) + (1-\gamma)S_{t-M} \tag{5}$$

$$\hat{Y}_{t+1} = (L_t + k.B_t)S_{t-M-k} \tag{6}$$

Additive Form

$$L_t = \alpha(Y_t - S_{t-M}) + (1-\alpha)(L_{t-1} + B_{t-1}) \tag{7}$$

$$B_t = \beta(L_t - L_{t-1}) + (1-\beta)B_{t-1} \tag{8}$$

$$S_t = \gamma(Y_t - L_t) + (1-\gamma)S_{t-M} \tag{9}$$

$$\hat{Y}_{t+1} = (L_t + k.B_t) + S_{t-M-k} \tag{10}$$

where M states the seasonal period (e.q. for monthly period M = 12) and k forecast horizon.

3.2.3. State space models (error-trend-seasonality)

Conventional exponential smoothing models are inadequate to handle nonstationary time series due to their linear structure. To fix the inadequacy state space models (ETS) that combine standard exponential smoothing methods with dynamic nonlinear model structures have been developed [49]. ETS models have state equations that describe the change of unobservable components (level, trend, seasonality) in time. The 30 model combinations within the ETS framework can be grouped into two main groups based on whether the error terms in the equations are additive or multiplicative [48] (see Table 4).

3.2.4. Trigonometric seasonality, Box–Cox transformation, ARMA errors, trend components, seasonal components (TBATS) models

The classical forecast approach runs weak performance depending on univariate forecasting problems and complex seasonality. Wider seasonality periods, non-integer seasonality, calendar effect, non-nested seasonality, and violation of the autocorrelation assumption are the main factors causing the poor performance of forecasting models. The evolution of TBATS models starts with the incorporation of a second seasonal component into the HW models. However, when the seasonal periods are extensive, this modified approach encounters difficulties in calculating the initial value. The modified model was enhanced and the BATS model was achieved by including Box–Cox transformation and ARMA errors, with the addition of T seasonal patterns. The BATS models are effective in handling time series data with multiple seasonal patterns, but they cannot produce proper results when the seasonality is non-integer. Additionally, the BATS models face initial value calculation challenges. The issues related to forecasting were resolved by replacing the seasonal component with a trigonometric form. In Eqs. (11) and (12), Y_t represents the electricity production data.

$$Y_t^{(\omega)} = \begin{cases} Y_t^{(\omega)} - 1/\omega, & \omega \neq 0 \\ logY_t, & \omega = 0 \end{cases} \tag{11}$$

$$Y_t^{(\omega)} = L_{t-1} + \phi B_{t-1} + \sum_{i=1}^{T} S_{t-m_i}^{(i)} + d_t \tag{12}$$

$$L_t = L_{t-1} + \phi B_{t-1} + \alpha d_t \tag{13}$$

$$B_t = (1-\phi)B + \phi B_{t-1} + \beta d_t \tag{14}$$

$$d_t = \sum_{i=1}^{p} \varphi d_{t-i} + \sum_{i=1}^{q} \theta_i \epsilon_{t-i} + \epsilon_t \tag{15}$$

$$S_t^{(i)} = \sum_{j=1}^{k_i} S_{j,t}^{(i)}; S_{j,t}^{(i)} = \begin{cases} S_{j,t-1}^{(i)} cos\lambda_j^{(i)} + S_{j,t}^{*(i)} sin\lambda_j^{(i)} + \gamma_1^{(i)} d_t \\ -S_{j,t-1}^{(i)} sin\lambda_j^{(i)} + S_{j,t}^{*(i)} cos\lambda_j^{(i)} + \gamma_2^{(i)} d_t \end{cases} \tag{16}$$

Eq. (11) through (15) show the TBATS model. The parameter ω represents the Box–Cox transformation, ϕ represents the damping parameter, and d_t represents the ARMA (p, q) process. The values $m_1, m_2, \ldots, m_T$ represent seasonal periods, while ϵ_t represents the white noise error term, whereas α, β, $\gamma_1^{(i)}$ and $\gamma_2^{(i)}$ are smoothing parameters and $\lambda_j^{(i)} = 2\pi/m_i$ for $i = 1, 2, \ldots, T$. The seasonal component of the BATS model was transformed into a trigonometric form using the Fourier series, as demonstrated in Eq. (16). The TBATS model is derived by integrating the $S_{t-m_i}^{i}$ for $i = 1, 2, \ldots, T$ component, which represents a trigonometric seasonal component.

In Eq. (16), $S_{(j,t)}^{(i)}$ represents the stochastic level of the i.th seasonal component and $S_{j,t}^{*(i)}$ represents the stochastic growth of the i.th seasonal component. The TBATS models have more parameters than the BATS models. They involve the analysis of managing seasonal components, which are nested or non-nested and nonlinear relationships. Additionally, the TBATS models can handle violations of the autocorrelation assumption [50].

3.2.5. The autoregressive distributed lag model

The ARDL model examines the relationship between the stationary and nonstationary dynamic variables [51]. The Engle–Granger cointegration method has long been used to investigate the connection among the variables. However, this method has an important disadvantage: The variables must be integrated in the same order for it to be applicable. The bounds test eliminates this requirement and allows variables to be integrated at level, first order or bilaterally integrated [52]. The ARDL bounds testing approach was used to examine the effects of variables affecting energy production and forecast performance. As in Eqs. (17) and (20), Y_t is the electricity production data and X_t presents the explanatory variables.

$$Y_t = \alpha + \delta T + \beta(B,p)Y_t + \sum_{i=1}^{k} \gamma_i(B,q_i)X_{it} + u_t \tag{17}$$

where

$$\beta(B,p)Y_t = Y_t(\beta_1 B + \beta_2 B^2 + \cdots + \beta_p B^p) \tag{18}$$

$$\gamma_i(B,q_i)X_{it} = X_{it}(\gamma_{i0}B^0 + \gamma_{i1}B + \cdots + \gamma_{iq_i}B_i^q) \tag{19}$$

Eq. (16) shows the general form of the ARDL model that includes intercept α and trend (T). Y_t denotes the dependent variable, X_t is the independent variable and B is the lag operator [45].

$$Y_t = \alpha + \phi Y_{t-1} + \sum_{i=1}^{k} \Omega_i X_{it-1} + \beta(B,p)\Delta Y_t + \sum_{i=1}^{k} \gamma_i(B,q_i)\Delta X_{it} + \varepsilon_t \tag{20}$$

Eq. (19) shows the conditional error correction model [52]. The conditional ECM has been estimated with a maximum of 12 lags to investigate the cointegration. The appropriate model combination was determined depending on an AIC and other diagnostic results. The cointegrated models were estimated using Eq. (16) during the training period of 2012M01-2021M05. The appropriate model combination was

determined using error correction estimation, and forecasts were generated for the test period of 2021M06-2022M05. As previously stated, the variables need to be integrated either at the level or first difference for the bound test approach. The ADF test results indicate that NG, GEO, BIO and CPI are I(2). Therefore these variables were excluded from the ARDL analysis. In the ARDL model, a comprehensive set of 66 models was estimated, encompassing distinct combinations of independent variables, all of which exhibit an I(1) or I(0) level.

3.3. Deep learning models

3.3.1. Artificial neural networks

ANNs are a machine learning technique that is non-parametric and inspired by the structure of the human brain [53]. They consist of interconnected artificial neurons organized into layers. Each neuron multiplies its inputs by weight and sums up the resulting products. The neuron then applies an activation function to this sum. The decision to transmit the signal to the next neuron depends on the output of this activation function. A single neuron, aka perceptron, [54] can be represented as

$$y = \phi\left(b_i + \sum_{i=1}^{n} w_i X_i\right) \tag{21}$$

where w_i is the weights, b_i is the bias, X_i is the inputs and ϕ is the activation function. If hidden layers are added to the model, it is called a multilayer perceptron and the output is calculated as follows [55]:

$$y = \psi\left(b_2 + \sum_{k=1}^{q} w_{ok}\theta\left(b_1 + \sum_{j=1}^{m} w_{kj}\phi\left(\ldots\delta\left(b_0 + \sum_{i=1}^{n} w_{li}X_i\right)\right)\right)\right) \tag{22}$$

Where ψ, θ, ϕ, δ, are activation functions, b_0, b_1, b_2 are bias terms, w_{ok} is the weight from neuron k in the last hidden layer to the output neuron o and n is the number of inputs.

ANNs are commonly trained using the backpropagation (BP) algorithm [56]. The objective of this algorithm is to find the weight parameters w that minimize the error between the predicted output of the network and the true output. First, the data are fed into the network and the predictions are generated using current weights and biases. Next, a loss function is computed based on the predicted and actual values. The gradient of the loss function with respect to the weights and biases is then calculated. The weights and biases are then updated based on this gradient value. These steps are repeated until a stopping criterion is met.

The deep learning models implemented in this study incorporated two hidden layers. The number of neurons within these layers was systematically varied, ranging from 20 to 100 with increments of 20, to assess their influence on the model's performance and behaviour.

3.3.2. Long short-term memory

LSTM [57] is a neural network structure frequently employed to forecast temporal relationships in diverse fields such as time series analysis, language modelling, speech recognition, and video analysis. One of the main advantages of LSTM is that it resolves the vanishing gradient problem that typically arises in practical applications of recurrent neural networks (RNN) [58].

LSTM achieves this by incorporating three gates that regulate the flow of information into and out of the cell state. These are the input gate, forget gate and output gate. The input gate determines which information to add to the cell state, while the forget gate determines which information to remove from the cell state. Finally, the output gate determines which information to output as the final hidden state. The equations for these components are as follows:

$$f_t = \sigma(W_f x_t + U_f h_{t-1} + b_f) \tag{23}$$

$$i_t = \sigma(W_i x_t + U_i h_{t-1} + b_i) \tag{24}$$

$$\tilde{C}t = \tanh(W_c x_t + U_c h_{t-1} + b_c) \tag{25}$$

$$C_t = f_t C_{t-1} + i_t \tilde{C}_t \tag{26}$$

$$o_t = \sigma(W_o x_t + U_o h_{t-1} + b_o) \tag{27}$$

$$h_t = o_t \tanh(C_t) \tag{28}$$

In this context, σ represents the sigmoid function. The forget gate is represented by f_t, the input gate by i_t, the output gate by o_t, the cell state by C_t, the candidate cell state by $\tilde{C}_t$, the hidden state by h_t, and the input at time step t by x_t. The weight matrices for the forget, input, cell state, and output gates are denoted as W_f, W_i, W_c, W_o, U_f, U_i, U_c, and U_o, respectively. The bias terms for the forget, input, cell state, and output gates are represented by b_f, b_i, b_c, and b_o, respectively.

3.3.3. Convolutional neural networks

CNNs [59] are neural network models specifically designed for image processing. Unlike standard ANNs, CNNs are equipped with convolution and pooling layers that play a crucial role in generating significant features from the input data and downsampling them, respectively. The convolution layer begins by creating a filter or kernel matrix, which is smaller than the input matrix. This filter is then moved throughout the entire input matrix using a sliding window approach. At each position, a dot product between the corresponding part of the input matrix and the filter is calculated, and this result is stored in the output matrix. The convolution layer formula can be expressed as

$$Y_{i,j} = \phi\left(\sum_{r=0}^{q}\sum_{c=0}^{q} W_{r,c}X_{i+r,j+c} + b\right) \tag{29}$$

The value of Y at the intersection of row i and column j in the feature map is denoted as $Y_{i,j}$. The corresponding value in the input matrix at row $i + c$ and column $j + r$ is represented as $X_{i+c,j+r}$. The activation function chosen for the operation is ϕ, while $W_{c,r}$ refers to the weight at row r and column c of the convolution kernel. Additionally, b denotes the bias associated with the convolution kernel.

In the pooling layer, a similar sliding window approach is used. However, instead of calculating the dot product, the maximum or average value, depending on the chosen pooling method, is extracted from the corresponding part of the input matrix, and this value is stored in the output matrix. These layers are then connected to a fully connected layer, and the final result is obtained.

3.4. Decomposition method

The STL is a method used to decompose a time series into its constituent parts, which are the trend, seasonal, and residual components. The main purposes of STL are to acquire accurate trend and seasonal components from data, unaffected by temporary and abnormal fluctuations, to identify variations in the trend and seasonal patterns, even in the presence of missing data points, and to provide a computationally simple approach for achieving this. The STL method uses the loess technique to decompose a time series that contains missing data points [60].

4. Empirical results, discussion, and policy implications

4.1. Empirical results

During the forecasting task, the datasets for univariate time series models are partitioned into two distinct subsets, namely the training set and the testing set. The training set comprises 113 observations, while the testing set encompasses 12 observations. In the context of deep learning and multivariate models, the dataset is subdivided into three distinct partitions: the training set, the validation set, and the

Table 5
Comparison of forecasting performances in terms of MAPE.

MAPE															
Methods\Dep. Vars.	TP	R_1	NG	R_2	HYD	R_3	COAL	R_4	WIND	R_5	FO	R_6	GEO	R_7	BIO	R_8
sARIMA	2.256	5	10.677	5	10.399	3	11.133	10	14.005	10	161.234	7	2.176	2	2.795	6
HW Add.	30.112	18	32.245	14	26.573	12	27.117	16	70.757	17	4573.984	16	88.667	18	88.686	18
HW Mult.	30.114	19	32.274	15	26.208	11	25.967	15	65.562	16	4856.845	17	88.616	17	88.675	16
ETS	1.931	3	11.126	6	12.222	6	9.399	6	12.702	8	240.211	10	2.423	4	2.989	7
TBATS	2.266	6	12.870	7	11.820	5	10.141	7	12.639	7	124.295	6	3.672	8	3.342	11
STL sARIMA	2.061	4	8.068	2	27.426	13	7.267	2	11.558	3	358.138	12	2.672	5	2.591	5
STL HW Add.	29.986	16	34.849	16	28.570	16	41.799	19	77.173	19	4001.268	15	87.688	15	88.580	15
STL HW Mult.	30.020	17	35.738	17	32.021	18	36.079	18	74.888	18	6990.744	18	88.139	16	88.686	17
STL ETS	1.630	2	8.647	4	11.013	4	8.102	4	11.798	4	557.871	14	4.108	9	2.071	2
ANN	5.565	12	27.837	12	24.916	10	14.967	14	16.871	13	230.728	9	54.991	14	2.535	4
LSTM	3.909	8	17.163	9	21.201	9	10.293	8	15.813	11	76.327	5	3.073	6	3.168	10
CNN	6.932	15	30.157	13	27.556	14	13.148	12	16.203	12	166.876	8	3.602	7	2.323	3
STL-ANN	5.746	13	38.923	18	64.845	19	28.076	17	30.789	15	9909.662	19	46.851	13	3.099	9
STL-LSTM	**1.626**	**1**	**4.710**	**1**	**9.131**	**1**	7.508	3	10.416	2	50.605	4	**2.087**	**1**	3.052	8
STL-CNN	5.507	11	15.017	8	10.365	2	**5.651**	**1**	**10.260**	**1**	337.959	11	2.391	3	**1.970**	**1**
MV-ANN	5.237	9	8.141	3	12.624	7	10.614	9	13.687	9	**25.630**	**1**	9.784	12	8.764	13
MV-LSTM	5.428	10	22.649	10	29.135	17	9.122	5	12.256	6	26.599	2	5.553	10	4.408	12
MV-CNN	6.744	14	26.405	11	27.702	15	13.423	13	17.599	14	27.891	3	5.854	11	11.760	14
ARDL	3.092	7	–	–	16.535	8	12.907	11	11.899	5	403.616	13	–	–	–	–

Table 6
Comparison of forecasting performances in terms of RMSE.

RMSE															
Methods\Dep. Vars.	TP	R_1	NG	R_2	HYD	R_3	COAL	R_4	WIND	R_5	FO	R_6	GEO	R_7	BIO	R_8
sARIMA	913 751.12	6	1 139 236.46	6	521 572.38	2	1 029 488.11	10	493 039.81	12	21 365.78	12	22 114.58	4	18 577.32	5
HW Add.	8 208 756.23	18	2 375 007.09	12	1 881 202.45	15	2 578 659.69	17	2 000 263.80	17	204 925.41	16	669 102.75	18	488 317.95	17
HW Mult.	8 209 098.75	19	2 378 610.69	13	1 885 107.68	16	2 492 406.83	16	1 883 015.62	16	226 518.17	17	668 736.55	17	488 313.58	16
ETS	685 157.90	3	1 076 001.60	5	731 128.41	6	823 964.87	5	396 433.69	7	28 695.25	13	**21669.65**	**1**	19 234.40	7
TBATS	764 333.54	5	1 161 169.17	7	691 392.20	5	995 496.11	9	386 006.08	5	13 971.39	8	30 402.71	7	22 751.61	11
STL sARIMA	745 459.53	4	867 285.51	3	1 485 190.44	9	736 196.38	3	333 149.09	3	16 426.27	9	22 959.35	5	15 310.00	3
STL HW Add.	8 183 556.32	16	2 514 486.95	16	2 143 231.50	17	3 568 359.72	18	2 150 919.12	19	191 951.99	15	661 968.63	15	487 804.09	15
STL HW Mult.	8 191 132.83	17	2 586 084.00	17	2 570 715.75	18	3 618 517.38	19	2 085 588.84	18	363 411.33	18	665 200.35	16	488 424.22	18
STL ETS	675 535.14	2	882 908.73	4	638 401.06	3	750 137.11	4	341 218.40	4	29 167.54	14	34 101.62	8	**13104.37**	**1**
ANN	1 927 761.01	12	2 079 752.84	10	1 683 689.74	13	1 233 063.62	14	509 479.98	13	9655.83	6	414 717.02	13	19 865.29	8
LSTM	1 510 685.04	8	1 864 405.09	9	1 500 310.20	11	875 692.17	7	456 275.50	10	4233.47	5	29 171.85	6	19 895.81	9
CNN	2 466 245.41	14	2 418 548.76	14	1 672 879.61	12	1 106 565.69	11	475 691.06	11	10 820.47	7	35 437.26	9	16 427.11	4
STL-ANN	1 900 929.18	11	3 330 083.65	18	2 984 625.73	19	2 466 661.75	15	873 603.19	15	503 644.88	19	434 638.27	14	21 384.69	10
STL-LSTM	**658 631.01**	**1**	**529 114.79**	**1**	**450 055.91**	**1**	692 132.85	2	328 496.68	2	2819.44	4	22 039.58	**3**	18 747.22	6
STL-CNN	1 707 045.35	9	1 276 826.33	8	668 990.38	4	**587 652.99**	**1**	**304 431.79**	**1**	20 128.43	10	21 767.18	2	13 590.72	**2**
MV-ANN	1 777 953.65	10	800 184.55	2	752 800.60	7	957 319.22	8	421 916.87	8	**1737.21**	**2**	90 018.30	12	57 790.30	13
MV-LSTM	2 052 424.34	13	2 236 366.27	11	1 485 294.29	10	867 886.54	6	422 322.74	9	**1736.25**	**1**	47 728.99	10	35 695.84	12
MV-CNN	2 575 039.62	15	2 448 351.73	15	1 710 790.62	14	1 176 451.26	13	520 574.57	14	1810.02	3	56 465.40	11	68 785.25	14
ARDL	966 048.84	7	–	–	934 517.32	8	1 161 091.67	12	390 785.65	6	20 421.25	11	–	–	–	–

testing set. The training set encompasses 101 observations, whereas the validation set and the testing set comprise 12 observations each.

Tables 5 and 6 present the mean absolute percentage error (MAPE) and root mean square error (RMSE) loss functions and their ranks R_i as metrics for evaluating and comparing the forecasting performance of the models on unseen data points. As seen in Tables 5 and 6 present a comparison of the forecasting performance of 19 different forecasting models. Nevertheless, as the ARDL model necessitates variables to be either integrated of order zero or one, the corresponding values are left blank for certain series that are classified as integrated of order two. The objective is to assess the adequacy of the forecasting performance by comparing it with other models, specifically focusing on variables where the ARDL method can be appropriately applied.

The MAPE results, as presented in Table 5, reveal that hybrid deep learning models exhibit superior forecasting performance across all target variables, except for FO. Multivariate deep learning methods yield the most successful models for FO. Among the hybrid deep learning models, STL-LSTM demonstrates optimal performance for four variables, while STL-CNN performs optimally for three variables. The rank-order analysis of model performance suggests that hybrid approaches employing univariate time series models demonstrate performance that is on par with deep learning models.

The RMSE results displayed in Table 6 exhibit a notable similarity to the MAPE results in relation to the forecasting performance of the models. Nevertheless, the univariate time series models outperform the deep learning models in terms of forecasting performance for the GEO and BIO variables.

The internal evaluation of the multivariate (MV) models' outcomes reveals that the best performance was acquired from the FO variable in terms of both MAPE and RMSE. The observed situation can be attributed to the significant shift in the use of FO to produce electricity.

Based on Fig. 3, a substantial quantity of FO was used during the period from mid-2012 to mid-2016, albeit in a volatile manner. However, the usage of FO's decreased considerably during the subsequent periods. The decrease observed in the FO has been thought to have

adversely affected the efficacy of univariate forecasting approaches, implying that the use of multivariate methods yields superior outcomes when forecasting this variable.

Figs. 5 and 6 present the superior performance of various models in terms of MAPE and RMSE metrics, out of a total of 18 different models evaluated. The outcomes indicate that the proposed deep learning models based on the STL exhibit remarkable performance overall. Specifically, the STL-LSTM model stands out as the most preferred model, demonstrating excellent results in terms of MAPE for variables such as TP, NG, HYD, and GEO. However, the ETS model shows a negligible difference and is chosen as the best model for RMSE in the case of GEO. The primary reason for the high forecasting accuracy of the ETS model is the seasonality exhibited by the GEO data. Similarly, the STL-CNN model achieves optimal outcomes for both loss functions related to the COAL and WIND variables. In the case of BIO, the STL-CNN model is selected based on MAPE, while the STL-ETS model performs the best in terms of RMSE. The main reason for the best performance of the STL-ETS model within the BIO data is the presence of a sharp trend in the series. Consequently, decomposing the series by removing the trend and separately modelling each component has contributed to the improvement in forecasting accuracy. Lastly, the MV-ANN model outperforms all other models in both loss functions concerning FO.

4.2. Discussion, and policy implications

This paper investigates the forecasting accuracy of comprehensive forecasting models for electricity production from both renewable and non-renewable sources. In terms of the overall electricity production, the results have been evaluated comparatively for the upcoming 14-month period, considering the respective contributions of various energy sources to the production of electricity. The plots illustrating previously unseen values and the forecasted values have been generated using the STL-based LSTM hybrid model approach, which demonstrates superior model performance. Moreover, the same plots present the results for the forecasted values for the upcoming 14 months. Based on Figs. 7 and 8, this paper sets out several policy implications.

The projection indicates that the proportion of electricity production derived from the NG sources in the overall production will average approximately 22% during the initial ten months. However, for the subsequent 14-month period, this share is anticipated to rise to an average of 28% of the TP. Likewise, an analysis reveals that the proportion of electricity production from hydro-based sources in the overall production will experience an increase from 16% during the initial 10-month period to 20% in the subsequent 14-month period. Furthermore, the average contributions of FO, WIND, BIO, and GEO sources to the total electricity production during the initial ten-month period remain, on average, consistent with their shares in the subsequent 14-month period. One notable finding is the average share of electricity produced from coal in Türkiye, which is forecast to decrease from 36% during the initial ten-month period to 29% for the subsequent 14-month period. This trend indicates the progress in efforts to increase the share of electricity production from renewable energy sources in Türkiye, along with advancements in technological infrastructure. To enhance electricity production from renewable energy sources in Türkiye, it is crucial to give priority to the development of renewable energy, set long-term goals for renewable energy deployment, and promote partnerships between the public and private sectors to expedite the shift towards a sustainable energy system.

5. Conclusion

A hybrid approach combining a decomposition method and both deep learning and time series models is employed to forecast electricity production derived from various renewable energy sources. By incorporating the STL method and both deep learning and time series models, this hybrid model enhances the precision and reliability of forecasts. When dealing with multivariate models, the aim is to enhance the forecasting accuracy of the models by using seven distinct input variables. In this regard, the deep learning models have achieved success for certain target variables. However, the selection of variables to be included as inputs in the models is subject to the availability of data and the discretion of the researcher, which poses a limitation in terms of the generalizability of the study. Therefore, the main contribution of the proposed hybrid approach in this study is to prevent arbitrary selection of input variables in the model and provide an effective approach for understanding and modelling the behaviours of components related to the target variables.

The performances of the hybrid models such as time series models, deep learning models and multivariate models have been evaluated for forecasting electricity production. During the performance evaluation, the hybrid models were compared with 11 different models in terms of forecasting accuracy on the test set. The conclusions drawn from the experimental results are as follows:

- The hybrid models demonstrate superior performance compared to all other forecasters in terms of RMSE and MAPE metrics.
- The proposed hybrid model not only helps prevent time delays in obtaining any explanatory variables during the modelling stage but also effectively handles volatile or noisy data, which can pose challenges for the performance of multivariate models.
- The multivariate models in the context of deep learning models excel when dealing with datasets containing interacting variables and complex dependencies. They explicitly capture relationships among variables, leading to a comprehensive forecasting approach.

Accurate forecasts provide policymakers with valuable insights into future renewable energy production. This knowledge aids in directing investments towards research and development endeavours focused on advancing renewable energy technologies, energy storage solutions, grid management systems, and forecasting methodologies. Policies can endorse and stimulate innovation while fostering cooperation among academia, industry, and government bodies. Such joint undertakings expedite the progression towards a sustainable and eco-friendly energy landscape.

Furthermore, particularly in the past year, the disparity between electricity supply and demand in Türkiye has widened significantly, mainly due to economic challenges. As a result, accurate electricity production forecasts provide utilities and grid operators with the ability to strategically plan and oversee electricity generation from various energy sources to align with expected demand. This proactive coordination serves to reduce discrepancies and guarantees a reliable power supply. In pursuit of this objective, the study's findings could offer valuable insights into the decision-making process regarding the activation or deactivation of specific power plants and energy sources, thereby optimizing resource allocation.

Future research endeavours will strive to enhance the predictive efficacy of multivariate models through the integration of arbitrary input selection techniques within deep learning frameworks. The primary objective is to mitigate potential reductions in forecast performance that may emerge from such selection processes. This pursuit entails augmenting the model with components derived from diverse decomposition methodologies or forecasts generated by univariate time series models, thereby promising the model's overall forecasting performances.

Moreover, in future research, the price variable can be utilized as an input for daily-based forecasting of electricity production from different energy sources. This is particularly relevant because electricity prices significantly influence the economic feasibility of various energy

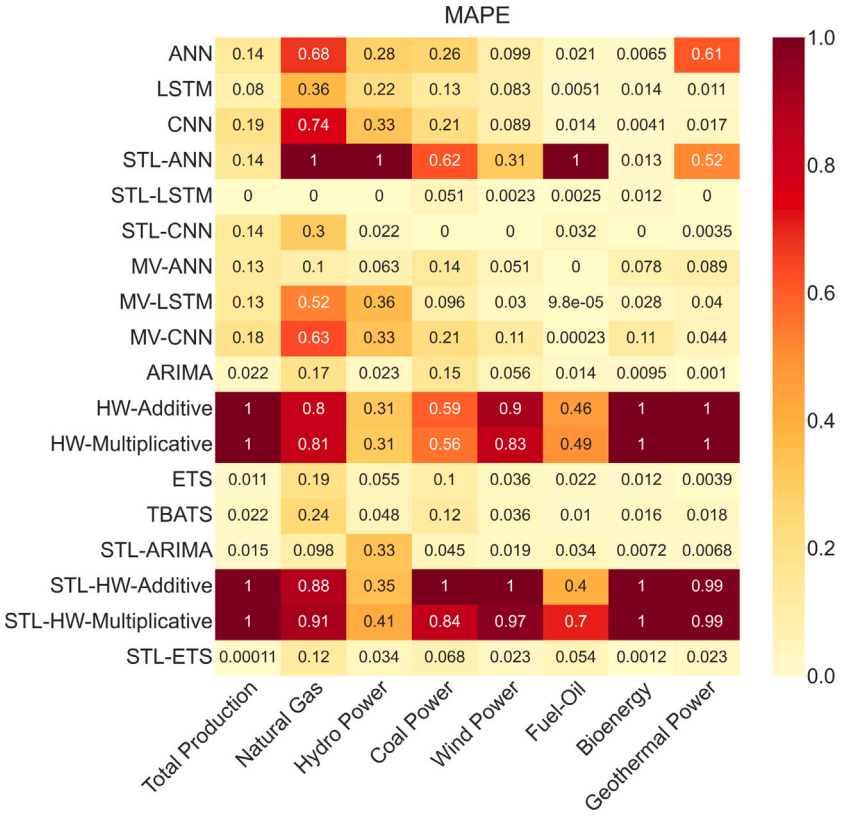

Fig. 5. Heatmap of MAPE. Note: Each column is normalized using min-max normalization.

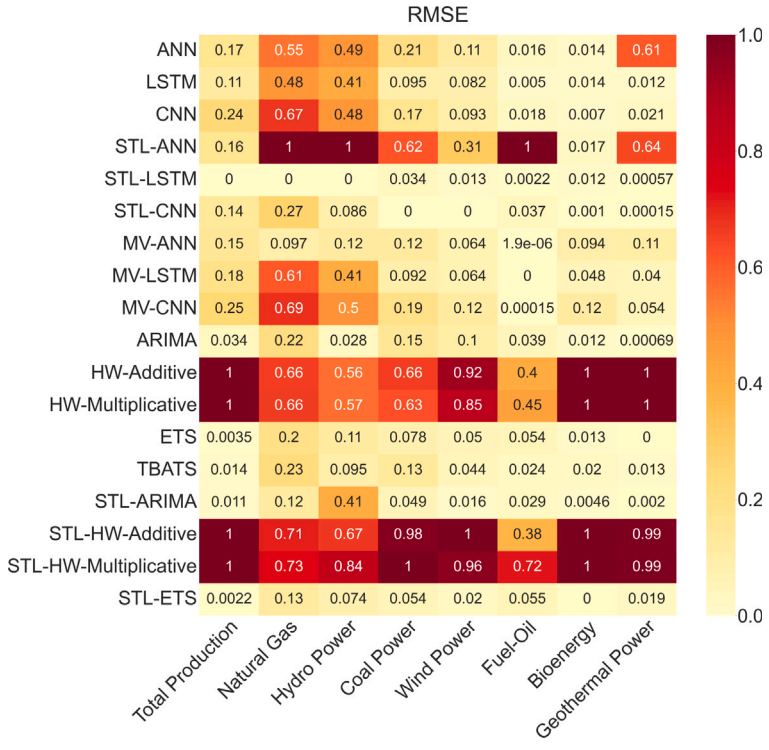

Fig. 6. Heatmap of RMSE. Note: Each column is normalized using min-max normalization.

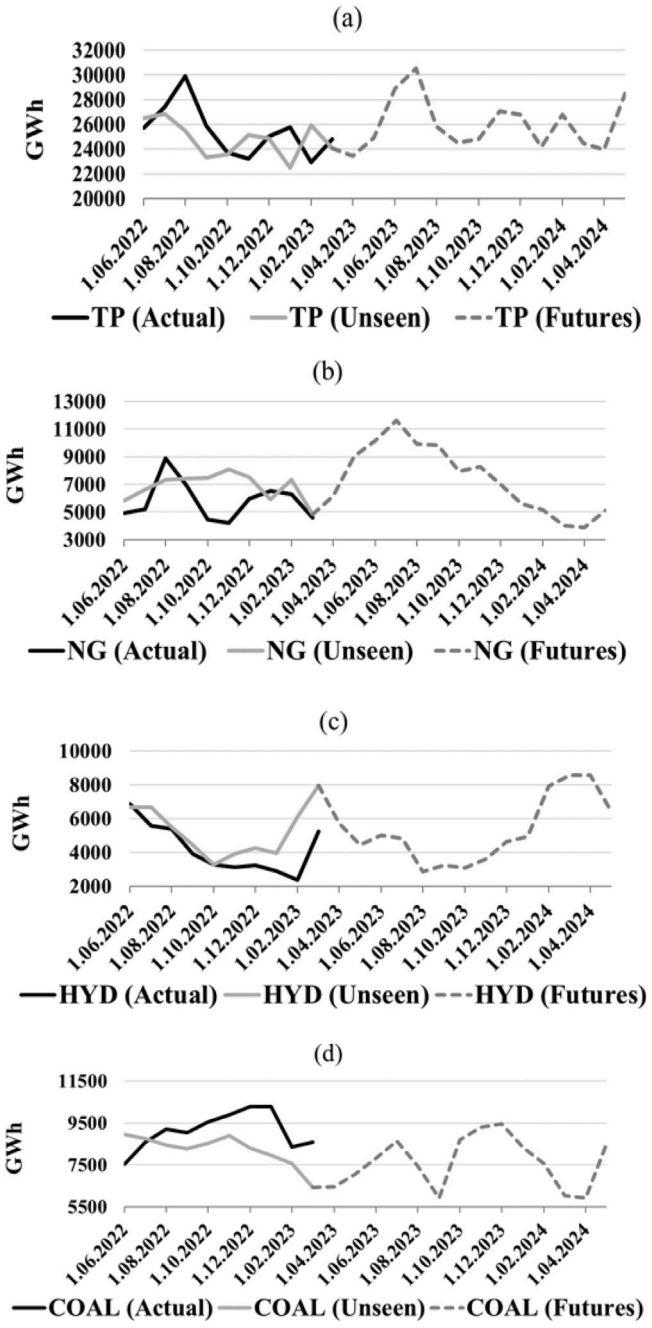

Fig. 7. (a) TP, (b) NG, (c) HYD, (d) COAL.

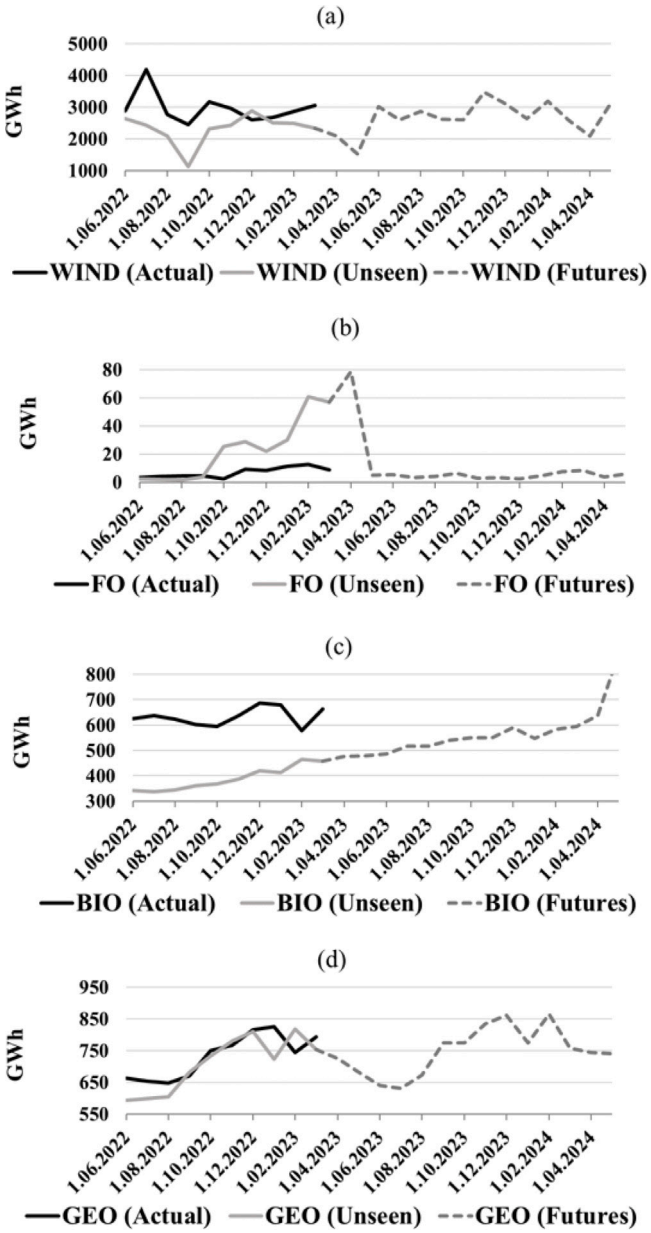

Fig. 8. (a) WIND, (b) FO, (c) BIO, (d) GEO.

sources. Firstly, considering the relationship between electricity production and electricity prices, different dynamic econometric models can be used to forecast electricity production from various energy sources. Afterwards, it is possible to model the forecast errors, which signify the differences between the forecasted electricity production and the actual electricity production values, utilizing a range of machine learning algorithms. The choice of algorithms, such as Random Forest and eXtreme Gradient Boosting (XGBoost), should be determined by the distinct characteristics of the data, the computational resources at hand, and the intended forecasting objectives, all with the aim of improving the accuracy of the forecasts. Another approach is to include the price variable as an input in both econometric models and machine learning algorithms for generating electricity production forecasts. Subsequently, a dynamic combining algorithm can be developed. This algorithm assigns varying weights to forecasts produced by different models based on realized forecasts. It can even assign a weight of zero to forecasts obtained from models that do not contribute to forecast accuracy.

CRediT authorship contribution statement

Emrah Gulay: Supervision, Conceptualization, Methodology, Software, Validation, Data curation, Writing – original draft, Writing – review & editing, Visualization. **Mustafa Sen:** Investigation, Conceptualization, Resources, Data curation, Writing – review & editing. **Omer Burak Akgun:** Investigation, Conceptualization, Writing – review & editing.

Declaration of competing interest

The authors declare that they have no known competing financial interests or personal relationships that could have appeared to influence the work reported in this paper.

Data availability

Data will be made available on request.

Acknowledgements

This research is funded by the Dokuz Eylul University through the Department of Scientific Research Project with the project reference SBA-2022-2665.

References

[1] Rodríguez-Álvarez A, Orea L, Jamasb T. Fuel poverty and well-being: A consumer theory and stochastic frontier approach. Energy Policy 2019;131:22–32.
[2] Churchill SA, Smyth R. Ethnic diversity, energy poverty and the mediating role of trust: Evidence from household panel data for Australia. Energy Econ 2020;86:104663.
[3] Wang Q, Kwan M-P, Fan J, Lin J. Racial disparities in energy poverty in the United States. Renew Sustain Energy Rev 2021;137:110620.
[4] Nomanbhay S, Hussein R, Ong MY. Sustainability of biodiesel production in Malaysia by production of bio-oil from crude glycerol using microwave pyrolysis: a review. Green Chem Lett Rev 2018;11(2):135–57.
[5] Jamil R. Hydroelectricity consumption forecast for Pakistan using ARIMA modeling and supply-demand analysis for the year 2030. Renew Energy 2020;154:1–10.
[6] Kilian L. The economic effects of energy price shocks. J Econ Lit 2008;46(4):871–909.
[7] Kaytez F. A hybrid approach based on autoregressive integrated moving average and least-square support vector machine for long-term forecasting of net electricity consumption. Energy 2020;197:117200.
[8] Bilgili M, Pinar E. Gross electricity consumption forecasting using LSTM and SARIMA approaches: A case study of Türkiye. Energy 2023;284:128575.
[9] Kaytez F, Taplamacioglu MC, Cam E, Hardalac F. Forecasting electricity consumption: A comparison of regression analysis, neural networks and least squares support vector machines. Int J Electr Power Energy Syst 2015;67:431–8.
[10] Kim T-Y, Cho S-B. Predicting residential energy consumption using CNN-LSTM neural networks. Energy 2019;182:72–81.
[11] Li G, Ning Z, Yang H, Gao L. A new carbon price prediction model. Energy 2022;239:122324.
[12] Wang Y, Zhang C, Fu Y, Suo L, Song S, Peng T, et al. Hybrid solar radiation forecasting model with temporal convolutional network using data decomposition and improved artificial ecosystem-based optimization algorithm. Energy 2023;128171.
[13] Neshat M, Nezhad MM, Sergiienko NY, Mirjalili S, Piras G, Garcia DA. Wave power forecasting using an effective decomposition-based convolutional Bi-directional model with equilibrium Nelder-Mead optimiser. Energy 2022;256:124623.
[14] Yu L, Ma Y, Ma M. An effective rolling decomposition-ensemble model for gasoline consumption forecasting. Energy 2021;222:119869.
[15] Lin Y, Lu Q, Tan B, Yu Y. Forecasting energy prices using a novel hybrid model with variational mode decomposition. Energy 2022;246:123366.
[16] Raza MY, Lin B. Oil for Pakistan: What are the main factors affecting the oil import? Energy 2021;237:121535.
[17] Karakurt I, Aydin G. Development of regression models to forecast the CO2 emissions from fossil fuels in the BRICS and MINT countries. Energy 2023;263:125650.
[18] Akbal Y, Ünlü KD. A univariate time series methodology based on sequence-to-sequence learning for short to midterm wind power production. Renew Energy 2022;200:832–44.
[19] Coskun C. A time-varying carbon intensity approach for demand-side management strategies with respect to CO2 emission reduction in the electricity grid. Int J Glob Warming 2019;19(1–2):3–23.
[20] Abdel-Aal R, Al-Garni AZ. Forecasting monthly electric energy consumption in eastern Saudi Arabia using univariate time-series analysis. Energy 1997;22(11):1059–69.
[21] Chavez SG, Bernat JX, Coalla HL. Forecasting of energy production and consumption in Asturias (northern Spain). Energy 1999;24(3):183–98.
[22] Saab S, Badr E, Nasr G. Univariate modeling and forecasting of energy consumption: the case of electricity in Lebanon. Energy 2001;26(1):1–14.
[23] Milligan M, Schwartz M, Wan Y-h. Statistical wind power forecasting models: Results for US wind farms. Tech. rep. Golden, CO (United States): National Renewable Energy Lab.(NREL); 2003.
[24] Bianco V, Manca O, Nardini S. Electricity consumption forecasting in Italy using linear regression models. Energy 2009;34(9):1413–21.
[25] Bianco V, Manca O, Nardini S, Minea AA. Analysis and forecasting of nonresidential electricity consumption in Romania. Appl Energy 2010;87(11):3584–90.
[26] Zachariadis T. Forecast of electricity consumption in Cyprus up to the year 2030: The potential impact of climate change. Energy Policy 2010;38(2):744–50.
[27] Shi J, Qu X, Zeng S. Short-term wind power generation forecasting: Direct versus indirect ARIMA-based approaches. Int J Green Energy 2011;8(1):100–12.
[28] Yuan C, Liu S, Fang Z. Comparison of China's primary energy consumption forecasting by using ARIMA (the autoregressive integrated moving average) model and GM (1, 1) model. Energy 2016;100:384–90.
[29] Atique S, Noureen S, Roy V, Subburaj V, Bayne S, Macfie J. Forecasting of total daily solar energy generation using ARIMA: A case study. In: 2019 IEEE 9th annual computing and communication workshop and conference. IEEE; 2019, p. 0114–9.
[30] Keles D, Scelle J, Paraschiv F, Fichtner W. Extended forecast methods for day-ahead electricity spot prices applying artificial neural networks. Appl Energy 2016;162:218–30.
[31] Bedi J, Toshniwal D. Deep learning framework to forecast electricity demand. Appl Energy 2019;238:1312–26.
[32] Titus J, Shah U, Siva Rama Sarma T, Jagyasi B, Gawade P, Bhagwat M, et al. Forecasting of electricity demand and renewable energy generation for grid stability. In: Proceedings of the 7th international conference on advances in energy research. Springer; 2021, p. 1571–81.
[33] Solyali D. A comparative analysis of machine learning approaches for short-/long-term electricity load forecasting in Cyprus. Sustainability 2020;12(9):3612.
[34] Ozbek A, Yildirim A, Bilgili M. Deep learning approach for one-hour ahead forecasting of energy production in a solar-PV plant. Energy Sources A Recov Utiliz Environ Effects 2022;44(4):10465–80.
[35] Ahmed A, Khalid M. A review on the selected applications of forecasting models in renewable power systems. Renew Sustain Energy Rev 2019;100:9–21.
[36] Iwok I, Udoh G. A comparative study between the ARIMA-Fourier model and the Wavelet model. Am. J. Sci. Ind. Res. 2016;7(6):137–44.
[37] Kumar J, Kaur A, Manchanda P. Forecasting the time series data using ARIMA with wavelet. J Comput Math Sci 2015;6(8):430–8.
[38] Conejo AJ, Plazas MA, Espinola R, Molina AB. Day-ahead electricity price forecasting using the wavelet transform and ARIMA models. IEEE Trans Power Syst 2005;20(2):1035–42.
[39] Rubio L, Alba K. Forecasting selected Colombian shares using a hybrid ARIMA-SVR model. Mathematics 2022;10(13):2181.
[40] Panigrahi S, Behera HS. A hybrid ETS–ANN model for time series forecasting. Eng Appl Artif Intell 2017;66:49–59.
[41] Chen Y, Tan H. Short-term prediction of electric demand in building sector via hybrid support vector regression. Appl Energy 2017;204:1363–74.
[42] Zhu B, Han D, Wang P, Wu Z, Zhang T, Wei Y-M. Forecasting carbon price using empirical mode decomposition and evolutionary least squares support vector regression. Appl Energy 2017;191:521–30.
[43] Wang K, Qi X, Liu H. A comparison of day-ahead photovoltaic power forecasting models based on deep learning neural network. Appl Energy 2019;251:113315.
[44] Pawar P, TarunKumar M, et al. An IoT based Intelligent Smart Energy Management System with accurate forecasting and load strategy for renewable generation. Measurement 2020;152:107187.
[45] Gulay E, Duru O. Hybrid modeling in the predictive analytics of energy systems and prices. Appl Energy 2020;268:114985.
[46] Box G, Jenkins G, Reinsel G, Ljung G. Time series analysis forecast and control. Wiley; 2016.
[47] Chatfield C. The analysis of time series an introduction. Chapman & Hall CRC; 1995.
[48] Hyndman R, Koehler A, Ord K, Snyder R. Forecasting with exponential smoothing: The state space approach. Springer; 2008.
[49] Wang Y, Xu C, Ren J, Wu W, Zhao X, Chao L, Liang W, Yao S. Secular seasonality and trend forecasting of tuberculosis incidence rate in China using the advanced error-trend-seasonal framework. Infect Drug Resist 2020;13:733–47.
[50] De Livera A, Hyndman R, Snyder R. Forecasting time series with complex seasonal patterns using exponential smoothing. J Amer Statist Assoc 2011;106(496):1512–27.
[51] Madziwa L, Pillalamarry M, Chatterjee S. Gold price forecasting using multivariate stochastic model. Resour Policy 2022;76:102544. http://dx.doi.org/10.1016/j.resourpol.2021.102544, URL https://www.sciencedirect.com/science/article/pii/S0301420721005511.
[52] Pesaran MH, Shin Y, Smith RJ. Bounds testing approaches to the analysis of level relationships. J Appl Econometrics 2001;16(3):289–326. http://dx.doi.org/10.1002/jae.616.
[53] Mcculloch W, Pitts W. A logical calculus of ideas immanent in nervous activity. Bull Math Biophys 1943;5:127–47.
[54] Rosenblatt F. The perceptron: a probabilistic model for information storage and organization in the brain. Psychol Rev 1958;65 6:386–408.

[55] Haykin S. Neural networks: A comprehensive foundation. international ed. Prentice Hall; 1999.
[56] Rumelhart DE, Hinton GE, Williams RJ. Learning representations by back-propagating errors. Nature 1986;323:533–6.
[57] Hochreiter S, Schmidhuber J. Long short-term memory. Neural Comput 1997;9(8):1735–80.
[58] Bengio Y, Simard P, Frasconi P. Learning long-term dependencies with gradient descent is difficult. IEEE Trans Neural Netw 1994;5(2):157–66.
[59] Lecun Y, Bottou L, Bengio Y, Haffner P. Gradient-based learning applied to document recognition. Proc IEEE 1998;86(11):2278–324.
[60] Cleveland R, Cleveland W, McRae J, Terpenning I. STL: A seasonal-trend decomposition procedure based on loess. J Off Stat 2011;106:1512–27.